

Development of a Laser Range Finder for 3D Map-Building in Rubble

— The 2nd Report: Development of the 2nd Prototype —

Masamitsu Kurisu
*Dpt. of Mechanical Engineering
College of Engineering
Tokyo Denki University
Tokyo 101-8457, Japan
kurisu@cck.dendai.ac.jp*

Yasuyoshi Yokokohji
*Dpt. of Mechanical Engineering
Graduate School of Engineering
Kyoto University
Kyoto 606-8501, Japan
yokokoji@mech.kyoto-u.ac.jp*

Yusuke Oosato
*Dpt. of Mechanical Engineering
College of Engineering
Tokyo Denki University
Tokyo 101-8457, Japan*

Abstract—In order to search and rescue the victims in rubble effectively, a 3D map of the rubble is required. As a part of the national project of rescue robot system, we are investigating a method for constructing a 3D map of rubble by teleoperated mobile robots. In previous work, we have developed the first prototype of laser range finder for rubble measurement. The developed one consists of a ring laser beam module and an omnivision camera. However, the first prototype has the weakness in which the measurement can be performed only in a dark place, because it is difficult to extract the reflected laser image from the picture captured in a light place. On the contrary, the pictures, in which the contrast of brightness is clarified, are required in order to extract the environmental features which are utilized for the position estimation of the robot based on the SLAM frame work. Also, the texture images captured in a light place are required for constructing virtualized rubble. In this paper, the second prototype of laser range finder which we developed in order to solve above dilemma is described. Although the concept of this prototype is similar to the first one, it has an infrared laser module and two cameras for capturing the reflected laser image and texture image separately. And, a hot mirror is used to dissociate the infrared laser ray from visible rays. We evaluate the measurement accuracy of the second prototype based on the measurement error analysis described in previous work. Using the second laser range finder, 3D maps of rubble were actually built with reasonable accuracy.

Index Terms—Laser Range Finder, Map Building, Rescue

I. INTRODUCTION

In order to search and rescue the victims in rubble effectively, a 3D map of the rubble is required. The constructed 3D map would be useful for finding a best route for helping the victim out and navigating the robots to some desired locations in the rubble. The authors are investigating a method for constructing a 3D map of rubble by teleoperated mobile robots with a motion canceling camera system, as a part of the special project for earthquake disaster mitigation in urban areas (DDT project for short) sponsored by the Ministry of Education, Culture, Sport, Science and Technology, Japan.

In mobile robot research, laser range finders are widely used for constructing a 2D map [1],[2],[3] and 3D map [4],[5],[6] of indoor environment. There are some works to construct a map inside a tunnel for underground mining [7]

and tunnel construction [8],[9]. The 3D maps built in the references [4],[5],[6],[9] are similar to the 3D map which we aim at. In these researches, the 3D laser range finder which added the pan function to the commercial 2D laser scanner is used. However, constructing a 3D map of rubble requires the following unique specifications. (i) To construct a complete 3D map, whole circumference of the rubble around the robot must be measured, if possible, without any scanning mechanism due to the durability requirement. (ii) The range sensor should be compact so that it can be mounted on a mobile robot. (iii) The target range is relatively shorter than the typical specification of conventional range finders. If we assume a small tunnel where humans can pass through by crawling, the target range would be around 300 mm. (iv) The required accuracy is relatively low compared to the conventional use in manufacturing domain. Considering the purpose of the map, errors around 10 mm to 20 mm are acceptable.

The laser range finders used in previous works are somewhat too large for our purpose, although they have high accuracy. We concluded that none of the existing laser range finders can meet those specifications, and decided to develop a special purpose range finder by ourselves. In the previous work [10], we developed the first prototype of laser range finder for 3D map-building in rubble. The first prototype consists of a ring laser beam module and an omnivision camera. The ring laser beam is generated by using a conical mirror and it is radiated toward interior wall of the rubble around a mobile robot on which the laser range finder is mounted. The omnivision camera with hyperbolic mirror can capture the reflected image of the ring laser on the rubble. Based on the triangulation principle, a cross section range data is obtained. Continuing this measurement as the mobile robot moves inside the rubble, a 3D map is obtained. Fig. 1 illustrates the concept of the proposed measurement method. We analyzed the measurement error using the geometric model of the laser range finder and obtained an optimal dimension of the one. The first prototype was built based on this analysis. Experimental results showed that the actual

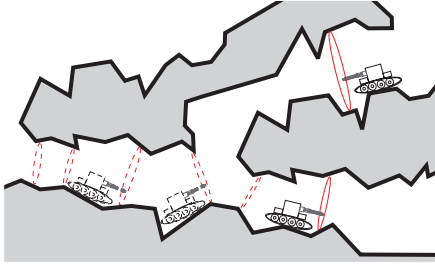


Fig. 1. Constructing a 3D map of rubble while searching victims

measurement errors were well matched to the theoretical values.

To build a 3D map, the position information of the range finder is needed. We are investigating a method to estimate the position of robot in the SLAM framework [11]. The method of extracting the environmental features for the SLAM from the picture captured by omnivision camera is also studied in our research project of position estimation. The first prototype has the weakness in which the measurement can be performed only in a dark place, because it is difficult to extract the reflected laser image from the picture captured in a light place. On the contrary, in order to extract the environmental features, the pictures, in which the contrast of brightness is clarified, are required. Additionally, we are investigating virtualized rubble, which can be obtained from mapping the texture image of rubble taken by the omnivision camera onto the constructed 3D map. To construct the virtualized rubble, the images captured in a light place are required. In order to solve this dilemma, we developed the second prototype of laser range finder.

In this paper, the developed second prototype is described. Although the concept of this prototype is similar to the first one, it has an infrared laser module and two cameras for capturing the reflected laser image and texture image separately. A hot mirror is used to dissociate the infrared laser ray from visible rays. The hot mirror is a special one which is built to reflect only an infrared ray, and transmit visible rays. We actually prototyped the second laser range finder which adopted a green laser module and half mirror instead of an infrared laser module and hot mirror, because production of the infrared laser module was too late for the deadline. We also evaluate the measurement accuracy of the second prototype based on the measurement error analysis described in [10]. Using the second laser range finder, 3D maps of rubble were actually built with reasonable accuracy.

The rest of this paper is organized as follows. In section II, the overview of the first prototype is shown. In section III, the details of the second one (the geometric model, principle of measurement, and measurement accuracy) are described. Experiments of constructing 3D maps by using the second laser range finder are shown in section IV. In section V, conclusion and future works are addressed.

II. THE FIRST PROTOTYPE LASER RANGE FINDER

Fig. 2 shows the first prototype which we have developed as a laser range finder for rubble measurement. Also, Fig.

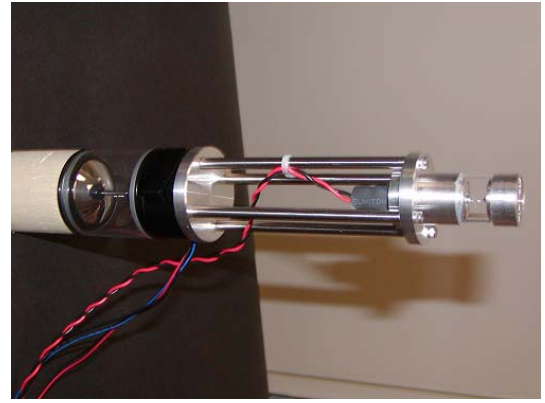


Fig. 2. Overview of the 1st prototype laser range finder

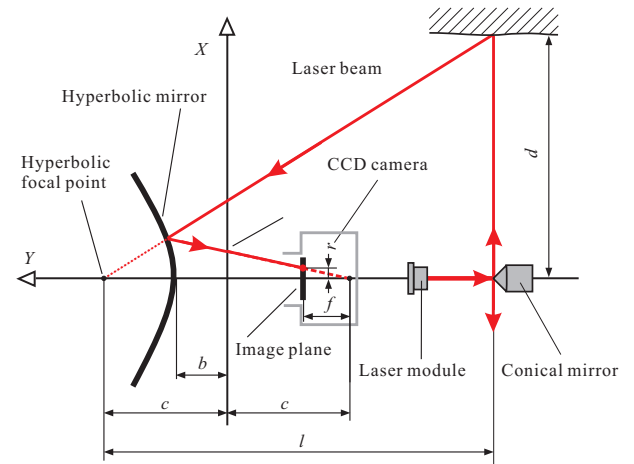


Fig. 3. Geometric model of the 1st prototype laser range finder

3 illustrates a geometric model of one. The first prototype consists of a laser module, a conical mirror, a hyperbolic mirror, and a CCD camera. The CCD camera is placed on the central axis of the mirror in such a way that its focal point coincides with the outer focal point of the mirror. The laser beam from the laser module reaches the conical mirror and reflects in 360-degree around the original laser beam. The ring laser image on the target surface is reflected on the hyperbolic mirror and captured by the CCD camera. In Fig. 3, d denotes the distance from the sensor to the target surface, l is the distance between the conical mirror (the starting point of the ring laser) and the focal point inside the hyperbolic mirror, and r is the distance of the laser image from the center on the image plane of the camera. Based on the triangulation principle, d can be obtained from r by using following equation,

$$d = \frac{(c^2 - b^2)lr}{(c^2 + b^2)f - 2bc\sqrt{f^2 + r^2}}, \quad (1)$$

where c is the focal point of hyperbolic mirror and b is shape parameters of the hyperboloid which is represented by

$$\frac{x^2}{c^2 - b^2} - \frac{y^2}{b^2} = -1, \quad (2)$$

and f is the focal length of the camera which is modeled as a pin-hole camera. From (1), once we measure the distance r on the image plane, we can get the distance to the target surface d . In order to get r , the ring laser image is extracted from the captured image using background subtraction technique and image filtering to remove image noises. The detail of the method for getting r from a captured image will be described in the next section.

The first prototype is compact in dimension, which are the diameter of 0.041 m and length of 0.2 m. And although required specification is not fulfilled, it has reasonable accuracy which is about 24×10^{-3} m measurement error in 0.3m measurement distance. However, the measurement can be performed only in dark surroundings. Even though using background subtraction technique, it is difficult to extract the ring laser image from the image captured in light surroundings. This is a weakness of the first prototype.

III. THE SECOND PROTOTYPE LASER RANGE FINDER

A. Geometric model

Fig. 4 illustrates a geometric model of the second prototype of laser range finder. The second prototype consists of an infrared laser module, a conical mirror, a hot mirror, a hyperbolic mirror, and two CCD cameras. The model is same as the one of the first prototype, except the hot mirror and two cameras. First camera is for capturing the laser image and second one for capturing a texture image. The image taken by the second camera is also used for extracting the environmental features which will be utilized for the position estimation based on SLAM frame work. The hot mirror is placed with its center on the origin of the coordinate frame. The ring infrared laser image on the target surface is reflected on the hyperbolic mirror and on the hot mirror. Then it is captured by the first camera through a hole which is holed at the top of the hyperbolic mirror. Also, the visible image of the target surface is reflected on the hyperbolic mirror, and passes through the hot mirror. Then it is captured by the second camera. According to this structure, we can get an infrared laser image and a visible image separately.

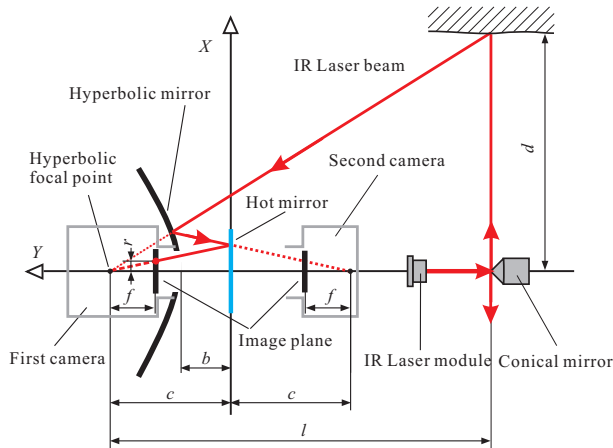


Fig. 4. Geometric model of the second prototype laser range finder

Fig. 5 shows the second laser range finder which we actually prototyped. Also, Fig. 6 shows the dimension of the prototyped range finder. We selected a camera with USB2 specification as the first camera. The selected camera can capture a progressive image at the frame rate up to 60 frames per second. The second camera is same as a camera used for the first prototype, which is a conventional NTSC standard camera with $512(H) \times 492(V)$ effective pixels. Hereafter, the first camera and second one are called USB2 camera and NTSC camera respectively. The hyperbolic mirror has a hole with 7mm diameter, and whose shape parameters are same as the one used for the first prototype. Since production of an infrared laser module was too late for the deadline, the green laser module is instead used for the range finder shown in Fig. 5. Also the half mirror is used instead of the hot mirror.

B. Measurement principle

The measurement principle in the second prototype is geometrically the same as the principle of the first prototype. Therefore, based on the triangulation principle, the distance from the sensor to the target surface d can be obtained from the distance r on the image plane by using (1). The procedure to get r from the captured image is described below. This procedure is also almost the same as the procedure for the first prototype.

The ring laser image is extracted from the captured image using background subtraction technique and image filtering to remove image noises. Fig. 7 shows an example of the laser image extraction. Fig. 7(a) shows the captured image when the sensor is put inside a rectangular box. Fig. 7(b) shows the extracted laser image after background subtraction and image filtering.

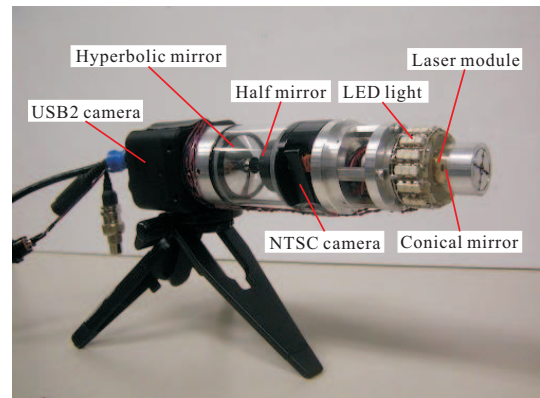


Fig. 5. Overview of the second prototype laser range finder

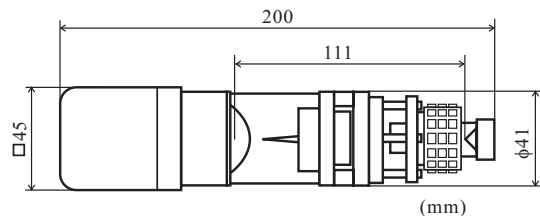


Fig. 6. Size of prototyped range finder

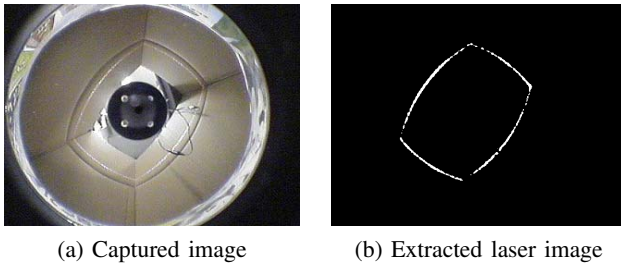


Fig. 7. Example of the laser image extraction

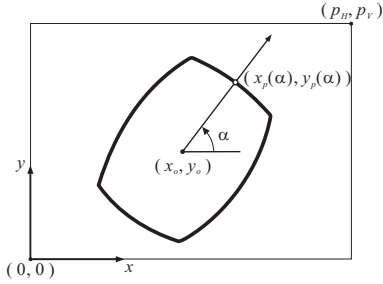


Fig. 8. Radial scanning of the laser image

Suppose that the effective number of pixels of the USB2 camera is $p_H \times p_V$ (pixel), the size of each pixel is $c_H \times c_V$ (m). An images taken by USB2 camera are directly converted into a digital image, namely the size of the captured image is $p_H \times p_V$ (dot). This property is one of the features of this USB2 camera.

The location of the laser image on the captured digital image is obtained by radial scanning as shown in Fig. 8, where $(x_o, y_o) = (p_H/2, p_V/2)$ (dot) denote the coordinates of the center of the captured image and (x_p, y_p) (dot) means the coordinates of the laser image on a radial scan line. Changing the angle of the scan line from the horizontal axis α step by step, we get the whole image. In our case, we change α every 1 deg and obtain 360 data points. Since the laser image has certain thickness, we calculate the center of gravity about image density of all the points on a scan line. This calculation is different from the calculation for the first prototype. In the first prototype, since the image was binarized before scanning, multiple points were detected on a single scan line. Then, we calculated the average of all the detected points.

The actual distance of the laser image from the center on the image plane, r (m), is given by

$$r = \sqrt{\{c_H(x_p - x_o)\}^2 + \{c_V(y_p - y_o)\}^2}. \quad (3)$$

From (1), once we measure the distance r on the image plane, we can get the distance to the target surface d .

C. Evaluation

The measurement period of the second prototype depends on the image processing and calculation mentioned above, which are performed by the software on a computer. The period on our computer with Pentium4[®] 3.06 GHz and 2GB memory is 128 msec.

After the calibration [10], we evaluated the accuracy of the sensor using square objects with sides 0.4, 0.5 and 0.6 m.

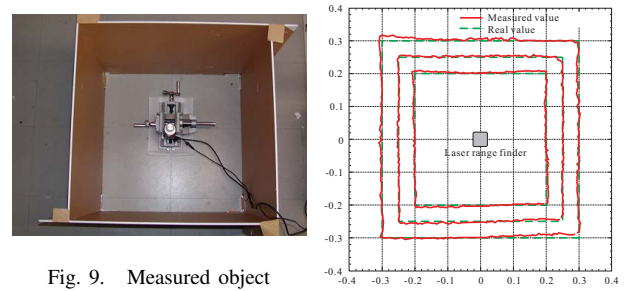


Fig. 9. Measured object

Fig. 10. Result of measurement

Fig. 9 shows the object with a side 0.6 m. Fig. 10 shows the measurement results.

From Fig. 10, one can see that the accuracy of the sensor is reasonably good. The longer the distance to the target is, the larger the error is. Fig. 11 illustrates the actual errors and the theoretical error curve. The theoretical error means the measurement error which calculated analytically in consideration of the quantization error in the digitized image. The minimum unit of the captured image is one dot, the quantization error could be ± 0.5 dot around the true value. Therefore, quantization error on the image plane Δr is given by

$$\Delta r = \sqrt{(c_H/2)^2 + (c_V/2)^2}. \quad (4)$$

From (1), the relation between the quantization error on the image plane Δr and the measurement error Δd is given by the following equation [10]:

$$\Delta d = \frac{(c^2 - b^2) \left\{ (b^2 + c^2) \sqrt{f^2 + r^2} f - 2bcf^2 \right\} l}{\sqrt{f^2 + r^2} \left\{ (b^2 + c^2) f - 2bc\sqrt{f^2 + r^2} \right\}^2} \Delta r. \quad (5)$$

The parameters used in the calculation are shown in Table I.

From Fig. 11, one can see that actual errors are well fitted to the theoretical error curve. The measurement is good until $d = 0.3$ m. Although the error becomes large in around 0.4 m distance, the required specification is fulfilled.

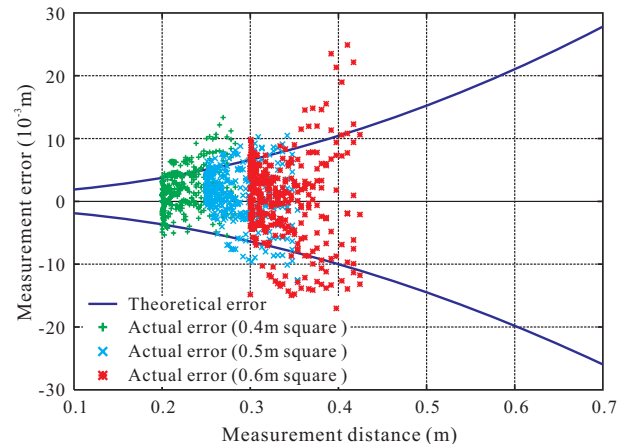


Fig. 11. Theoretical errors and actual ones

TABLE I
PARAMETERS USED IN THE CALCULATION

item	symbol	specification
effective pixels	$p_H \times p_V$	$656(H) \times 494(V)$
pixel size (10^{-6} m)	$c_H \times c_V$	$7.4(H) \times 7.4(V)$
focal length (10^{-3} m)	f	6.55
mirror parameter (10^{-3} m)	b	12.15
mirror parameter (10^{-3} m)	c	16.327

IV. EXPERIMENTS

A. Map building by manual positioning

We tried to build a 3-D map of rubble by the prototyped range finder. Fig. 12 shows the target rubble to be modeled. The target rubble consists of a rectangular box (0.45 m(W) \times 0.45 m(H) \times 0.45 m(D)) and some pieces of brick, stones, and ladders. Since the position estimation system was not implemented yet, we placed the sensor manually on the bottom of the box instead of a mobile robot as shown in Fig. 13. Fig. 14 shows the bottom plane of the box. In Fig. 14, a small circle and arrow mean the position and orientation of the sensor. Since the target rubble was measured fifteen times in total, fifteen cross sections were obtained.

Fig. 15 shows the measurement result, and Fig. 16 shows the constructed model by surface model. Fig. 17 also shows close-up views of the left side of the rubble and the corresponding part of the constructed model.

B. Map building by online measurement

We tried to build a 3-D map by online measurement. Fig. 18 shows the target environment, which is called *tunnel* hereafter.



Fig. 12. Measured environment for 3D model

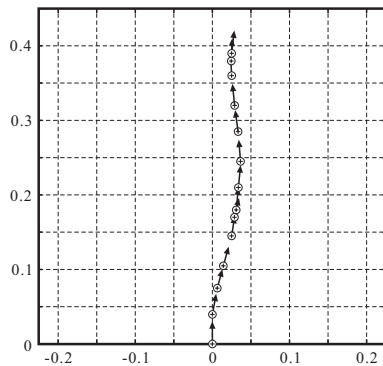


Fig. 14. Position and orientation of the sensor

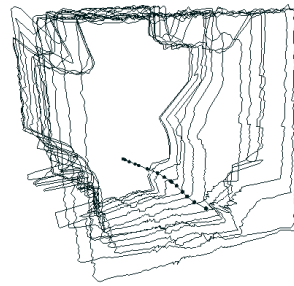


Fig. 15. Measurement result



Fig. 16. Constructed model



Fig. 17. Close-up views of the left side of the rubble and 3D model

The dimension of the *tunnel* is about 0.5 m(W) \times 0.35 m(H) \times 1 m(D). The sensor was mounted on a small robot as shown in Fig. 19. Then, we drove the robot straight forward at 0.2 m/sec speed in the *tunnel*. Since the time interval for measuring was 128 m/sec, the cross sections of the *tunnel* were measured with 26×10^{-3} m interval, forty times in total. Fig. 20 illustrates a snapshot during the measurement. Fig. 22 also shows the front view of the *tunnel*, and the corresponding view of the constructed model.

In this experiment, the position of the sensor was calculated based on the velocity of the robot and the time interval of measurement. Although the calculated position is not actual one, the constructed model represents the real environment with reasonable accuracy. In the practical use, the range finder is mounted on the mobile robot whose position cannot be measured directly when the robot is inside rubble. We are investigating a method to estimate the position of robot in the SLAM framework[11]. The method of extracting the environmental features for the SLAM from the picture captured by the NTSC camera is also studied in the research. Combining the result of the ongoing project with the range data obtained by the prototyped sensor is a future work.

V. CONCLUSION

In this paper, the second prototype of laser range finder for 3D map-building in rubble is described. The concept of the second prototype is similar to the first one. Since the sensor has also no moving parts like scanning mechanisms same as the first prototype, it is easy to make it durable in the actual rescue activities. The feature of the second prototype is that it has an infrared laser module and two cameras for capturing the reflected laser image and texture image separately. A hot mirror is used to dissociate the infrared laser ray from visible rays. We actually prototyped the second laser range



Fig. 18. Measured environment called tunnel

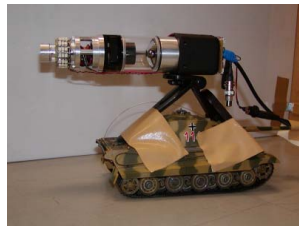


Fig. 19. Robot on which the sensor was mounted

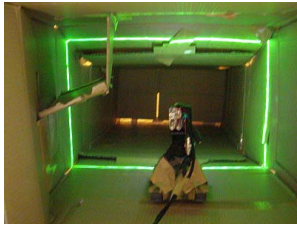


Fig. 20. Snapshot during the measurement

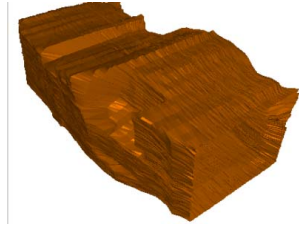


Fig. 21. Constructed model of the tunnel



Fig. 22. Front view of the tunnel and constructed model

finder by using a green laser module and half mirror instead of an infrared laser module and hot mirror, respectively. We evaluate the measurement accuracy of the prototyped sensor based on the measurement error analysis mentioned in previous work, and show that the actual measurement errors are well matched to the theoretical value. Using the second laser range finder, 3D maps of rubble were actually built with reasonable accuracy. However, it is necessary to verify the validity of the second prototype equipped with the infrared laser module and the hot mirror, although its effectiveness is already confirmed in some preliminary experiments.

As a future work, we will combine the result of our other research project of SLAM with this result and construct a 3D map of rubble by using a mobile robot that mounts this range finder. Also, we have to develop the fast constructing method of 3D map with the texture image of rubble taken by the omnivision camera. If we could map the texture image of rubble onto the constructed 3D map, immersible virtualized rubble can be obtained. This virtualized rubble would be useful for precise searching and rout planning and navigation.

ACKNOWLEDGMENT

This research was supported by the special project for earthquake disaster mitigation in urban areas (DDT project

for short) sponsored by the Ministry of Education, Culture, Sport, Science and Technology, Japan.

REFERENCES

- [1] B. Yamauchi, A. Schultz, and W. Adams: "Mobile Robot Exploration and Map-Building with Continuous Localization," *Proc. of the 1998 IEEE Int. Conf. on Robotics and Automation*, pp.3715–3720, 1998.
- [2] L. Zhang and B.K. Ghosh: "Line Segment Based Map Building and Localization Using 2D Laser Rangefinder," *Proc. of the 2000 IEEE Int. Conf. on Robotics and Automation*, pp.2538–2543, USA, 2000.
- [3] D. Hahnel, D. Fox, W. Burgard, and S. Thrun: "An Efficient FastSLAM Algorithm for Generating Maps of Large-Scale Cyclic Environments from Raw Laser Range Measurements," *Proc. of the IEEE/RSJ Int. Conf. on Intelligent Robots and Systems (IROS2003)*, pp.206–211, 2003.
- [4] Y. Liu, R. Emery, D. Chakrabarti, W. Burgard, and S. Thrun: "Using EM to Learn 3D Models with Mobile Robots," *Proc. of the Int. Conf. on Machine Learning (ICML)*, pp.329-336, 2001.
- [5] H. Surmann, A. Nuchter, and J. Hertzberg: "An Autonomous Mobile Robot with a 3D Laser Range Finder for 3D Exploration and Digitalization of Indoor Environments," *J. Robotics and Autonomous Systems*, pp.181–198, vol. 45, issues 3-4, ISSN 09218890, 2003.
- [6] I. Mahon and S. Williams: "Three-Dimensional Robotic Mapping," *Proc. of the Australasian Conf. on Robotics and Automation 2003*, 2003.
- [7] S. Scheding et al.: "Experiments in Autonomous Underground Guidance," *Proc. of the 1997 IEEE Int. Conf. on Robotics and Automation*, pp.1898–1903, 1997.
- [8] T.A. Melbye and R.H. Dimmock: "Modern Advances and Applications of Sprayed Concrete," *Proc. of the Int. Conf. on Engineering Developments in Shotcrete*, 2001.
- [9] S. Thrun et al. : "A System for Volumetric Robotic Mapping of Abandoned Mines," *Proc. of the 2003 IEEE Int. Conf. on Robotics and Automation*, pp.4270–4275, 2003.
- [10] M. Kurisu, Y. Yokokohji, Y. Shiokawa, and T. Samejima: "Constructing a 3-D Map of Rubble by Teleoperated Mobile Robots with a Motion Canceling Camera System," *Proc. of the IEEE/RSJ Int. Conf. on Intelligent Robots and Systems (IROS2004)*, pp.3118-3125, 2004.
- [11] Y. Yokokohji, M. Kurisu, T. Saida, Y. Kudo, K. Hayashi, and T. Yoshikawa: "Constructing a 3-D Map of Rubble by Teleoperated Mobile Robots with a Motion Canceling Camera System," *Proc. of the IEEE/RSJ Int. Conf. on Intelligent Robots and Systems (IROS2003)*, pp.3118-3125, 2003.